

If $3 \nmid \mu$ then $F_5 \leq U/2$. *Proof:* $3 \mid U+V$ because $F_2=3$. If $V=0$ then $3 \mid U$ and $F_5 \leq U/3$; if $V \neq 0$ then $F_5 \leq U/2$ because of (14). All the following lower limits on Σ can therefore be multiplied by 2 if $3 \nmid \mu$.

- (1) $F_3=1 \Rightarrow 2 \nmid \nu$ or $2 \nmid m+W$
 $\Rightarrow F_4 = \text{gcd}(\nu, W/3, m+W)$.
 (1.1) $W=0 \Rightarrow F_4 \leq m \Rightarrow G \leq 3mU$
 $\Rightarrow \Sigma \geq \Sigma_0/3 = (\mu\nu)^{1/2}$.
 (1.2) $W \neq 0 \Rightarrow F_4 \leq W/3 \Rightarrow G \leq WU$
 $\Rightarrow \Sigma \geq \Sigma_w > 6(\mu\nu)^{1/2}$.
 (2) $F_3=2 \Rightarrow F_4 = \text{gcd}(\nu/2, 2W/3, m+W)$.
 (2.1) $W=0, 4 \mid \nu \Rightarrow F_4 \leq m \Rightarrow G \leq 6mU$
 $\Rightarrow \Sigma \geq (\mu\nu)^{1/2}/2$.
 (2.2) $W=0, 4 \nmid \nu \Rightarrow F_4 \leq m/2 \Rightarrow G \leq 3mU$
 $\Rightarrow \Sigma \geq (\mu\nu)^{1/2}$.
 (2.3) $W \neq 0 \Rightarrow F_4 \leq 2W/3 \Rightarrow G \leq 4WU$
 $\Rightarrow \Sigma > 3(\mu\nu)^{1/2}/2$.

Case (c)

- $F_1 = F_2 = 1 \Rightarrow F_5 = \text{gcd}(\mu, 3U, U+V) \leq 3U/2$.
 (1) $F_3=1 \Rightarrow F_4 = \text{gcd}(\nu, 2W, m+W)$.
 (1.1) $W=0 \Rightarrow F_4 \leq m \Rightarrow G \leq 3mU/2$
 $\Rightarrow \Sigma \geq 2(\mu\nu)^{1/2}$.
 (1.2) $W \neq 0 \Rightarrow F_4 \leq 2W \Rightarrow G \leq 3WU$
 $\Rightarrow \Sigma > 2(\mu\nu)^{1/2}$.
 (2) $F_3=2 \Rightarrow F_4 = \text{gcd}(\nu/2, 2W, m+W)$.
 (2.1) $W=0, 4 \mid \nu \Rightarrow F_4 \leq m \Rightarrow G \leq 3mU$
 $\Rightarrow \Sigma \geq (\mu\nu)^{1/2}$.
 (2.2) $W=0, 4 \nmid \nu \Rightarrow F_4 \leq m/2 \Rightarrow G$
 $\leq 3mU/2 \Rightarrow \Sigma \geq 2(\mu\nu)^{1/2}$.

Acta Cryst. (1989). **A45**, 325–333

Electron Inelastic Plasmon Scattering and its Resonance Propagation at Crystal Surfaces in RHEED

BY Z. L. WANG,*† J. LIU AND J. M. COWLEY

Department of Physics, Arizona State University, Tempe, AZ 85287-1504, USA

(Received 26 September 1988; accepted 9 December 1988)

Abstract

The modified multislice theory [Wang (1989). *Acta Cryst.* **A45**, 193–199] has been employed to calculate the electron reflection intensity with and without considering the plasmon diffuse scattering in the geometry of reflection high-energy electron diffraction (RHEED). It has been shown that the inelastic scattering can greatly enhance the reflectance of a

* Present address: Cavendish Laboratory, University of Cambridge, Madingley Road, Cambridge CB3 0HE, England.

† To whom correspondence should be addressed.

$$(2.3) \quad W \neq 0, 4 \mid \nu \Rightarrow F_4 \leq 2W \Rightarrow G \leq 6WU$$

$$\Rightarrow \Sigma > (\mu\nu)^{1/2}.$$

$$(2.4) \quad W \neq 0, 4 \nmid \nu \Rightarrow F_4 \leq W \Rightarrow G \leq 3WU$$

$$\Rightarrow \Sigma > 2(\mu\nu)^{1/2}.$$

Summary

It follows from cases (a)–(c) that

$$\Sigma \geq \begin{cases} (\mu\nu)^{1/2}/2 & \text{if } 3 \mid \mu, 4 \mid \nu \\ 2(\mu\nu)^{1/2} & \text{if } 3 \nmid \mu, 4 \nmid \nu \\ (\mu\nu)^{1/2} & \text{otherwise.} \end{cases}$$

References

- BLERIS, G. L., NOUET, G., HAGÈGE, S. & DELAVIGNETTE, P. (1982). *Acta Cryst.* **A38**, 550–557.
 BONNET, R., COUSINEAU, E. & WARRINGTON, D. H. (1981). *Acta Cryst.* **A37**, 184–189.
 DELAVIGNETTE, P. (1982). *J. Phys. (Paris) Colloq.* **43**, C6, 1–13.
 DELAVIGNETTE, P. (1983). *J. Microsc. Spectrosc. Electron.* **8**, 111–124.
 ECKERLIN, P. & KANDLER, H. (1971). *Landolt-Börnstein, New Series, Group III*, Vol. 6. Berlin: Springer.
 FRANK, F. C. (1965). *Acta Cryst.* **18**, 862–866.
 GRIMMER, H. (1976). *Acta Cryst.* **A32**, 783–785.
 GRIMMER, H. & WARRINGTON, D. H. (1983). *Z. Kristallogr.* **162**, 88–90.
 GRIMMER, H. & WARRINGTON, D. H. (1985). *J. Phys. (Paris) Colloq.* **46**, C4, 231–236.
 GRIMMER, H. & WARRINGTON, D. H. (1987). *Acta Cryst.* **A43**, 232–243.
 HAGÈGE, S. & NOUET, G. (1985). *Scr. Metall.* **19**, 11–16.
 WARRINGTON, D. H. (1975). *J. Phys. (Paris) Colloq.* **36**, C4, 87–95.

reflection electron energy-loss spectroscopy (REELS) study of the 'true' resonance of GaAs (110) surface. This is considered as a characteristic of the resonance propagations of the electrons along the surface and may result from the generation of resonance radiation.

1. Introduction

The phenomenon of surface resonance has been observed in reflection high-energy electron diffraction (RHEED) for half a century (Kikuchi & Nakagawa, 1933). It has been variously termed 'surface state resonance', 'surface wave resonance' or 'surface resonance'. The theoretical investigations of the origin and the nature of the surface resonance have been approached in several ways.

A multislice approach has been developed assuming a two-dimensional periodicity, parallel to the surface (Maksym & Beeby, 1981). The crystal is considered to be cut into slices parallel to the surface and wave functions in different slices are connected by a transfer matrix. It has been shown that the resonance corresponds to the intrinsic bound states in the scattering potential of an atomic monolayer (Maksym & Beeby, 1982; Marten & Meyer-Ehmsen, 1985). When trapped in these states the electrons experience a planar channelling along the surface which is confined to the potential troughs of the topmost layers of the crystal due to a resonance-induced bandgap seen by the incident beam. In other words, the resonance effect can also be considered as a surface channelling phenomenon.

The Bethe theory is applied to surface calculations by assuming a three-dimensional periodic structure terminated by a plane (Colella, 1972). The calculations based on this approach (Bleloch, Howie, Milne & Walls, 1989) give some results contradictory to those obtained by Marten & Meyer-Ehmsen (1985). The results do not support the idea that under surface resonance conditions a significant component of the electron wave field is excited which is unusually strongly confined to the surface regions. The resonance effect is considered as bulk property instead of surface property.

An alternative multislice approach has been developed analogous to image simulation in the transmission case except that the slices are essentially nonperiodic since they are cut perpendicular to the crystal surface and include the wave function both inside and outside the crystals (Peng & Cowley, 1986; Wang, Lu & Cowley, 1987). The existence of the surface resonance wave has been predicted and observed directly in RHEED experiments (Wang, Liu, Lu & Cowley, 1989). The Goos-Hanchen effect (Kambe, 1988) has been predicted in RHEED calculations. The monolayer resonance characteristic of the electrons in RHEED has been found to be true

only at some specific conditions. In general, the electrons are accumulated on the surface top two to three atomic layers. This is in agreement with the experimental results of reflection electron energy-loss spectroscopy (REELS) (Wang *et al.*, 1987).

All the above approaches are based on elastic scattering theories; and some contradictory results are predicted. Thus it is not easy to get a clear theoretical picture. None of these calculations have taken into consideration the effects of electron inelastic scattering. This might be due to the lack of methods which are capable of including the inelastic scattering in the dynamical calculation for RHEED.

Recently, a new method has been introduced by Wang (1989*a*; Wang & Lu, 1988) to include the inelastic plasmon diffuse scattering (PDS) in the dynamical calculations for RHEED. This method is based on the multislice theory developed by Cowley & Moodie (1957). The inelastic energy loss is characterized as an interacting effective potential, which perturbs the wavelength of the electrons while traveling inside the crystal. Based on this approach, it has been shown that the inelastic scattering can significantly enhance the reflectance of a crystal surface (Wang, 1989*b*). The calculated intensity ratios for the elastically and the inelastically scattered electrons in RHEED are quantitatively in agreement with the measurements of REELS (Wang, 1989*c*).

The purpose of this paper, based on the developed inelastic scattering theory (Wang & Lu, 1988; Wang, 1989*a*), is to find the relationship between the electron inelastic scattering and the resonance propagation in crystal surfaces. The effect of the inelastic scattering in enhancing the reflection intensity in RHEED will be discussed. The predicted results will be compared with the RHEED and REELS observations.

2. Theory

For the convenience of the following discussion, it is necessary to review the modified multislice theory introduced by Wang (1989*a*). A related approach has been used by Cowley (1988) for high-resolution electron microscopy. The inelastic plasmon diffuse scattering (PDS) in the geometry of RHEED can be represented by an 'effective' potential U_{ef} , perturbing the wavelength of the electrons, resulting in an 'extra' term in the slice transmission function. In this approach, the modified transmission function for the n th slice in the multislice theory can be written as

$$q_n = \exp(i\sigma U_a \Delta z) \exp(i\sigma U_{ef} \Delta z), \quad (1)$$

where $\sigma = \pi/\lambda_0 V_0$, λ_0 is the wavelength of the initial incident electron with energy $E_0 = eV_0$. In (1), the first term is the phase grating resulting from the crystal potential (U_a), which is the same as that in the original multislice theory (Cowley & Moodie, 1957). The second term is a phase perturbation function arising

from the inelastic PDS, with

$$U_{ef} = -\Delta E(x, z)/e \\ = -\frac{1}{e} \int_0^z dz \int_0^\infty d\omega \int_0^{q_c} dq_y \hbar\omega \frac{d^2 P(\omega, q_y, x)}{d\omega dq_y}. \quad (2)$$

U_{ef} is derived for a planar interface formed by two semi-infinite media a and b by using the relativistic dielectric excitation theory (Garcia-Molina, Gras-Marti, Howie & Richie, 1985). A point electron travelling in medium b at distance x parallel to an interface with medium a has a differential probability per unit distance for energy loss ($\hbar\omega$) and momentum transfer ($\hbar q_y$), in the direction parallel to the interface and normal to the moving direction, given by

$$\frac{d^2 P(\omega, q_y, x)}{d\omega dq_y} = \frac{e^2}{2\pi^2 \varepsilon_0 \hbar v^2} \text{Im} \left[F(q_y, x) - \frac{1 - \beta^2 \varepsilon_b}{\varepsilon_b \alpha_b} \right], \quad (3)$$

where $\beta = v/c$; $\alpha_{a,b}^2 = q_y^2 + (\omega/v)^2(1 - \beta^2 \varepsilon_{a,b})$; v is the velocity of the electron; ε_a and ε_b are the dielectric constants of media a and b . The quantity $F(q_y, x)$ in (1) is given by

$$F(q_y, x) = \left[\frac{2\alpha_b^2(\varepsilon_a - \varepsilon_b)}{\varepsilon_a \alpha_b + \varepsilon_b \alpha_a} + (\alpha_a - \alpha_b)(1 - \varepsilon_b \beta^2) \right] \\ \times \frac{\exp(-2\alpha_b|x|)}{\varepsilon_b \alpha_b(\alpha_a + \alpha_b)}. \quad (4)$$

The electron wave function after being scattered by the n th slice can be written as

$$\psi_n = [\psi_{n-1} q_n] * P_n, \quad (5)$$

where $*$ denotes convolution, with P_n the propagation function of the n th slice for the electrons with energy E_0 , given to first-order approximation as

$$P_n = (i/\Delta z \lambda_0) \exp[-iK(x^2 + y^2)/2 \Delta z]. \quad (6)$$

The calculated results of (1) to (6) give the total contributions of the elastically and inelastically scattered electrons to RHEED. To compare the calculated total scattering with the calculations of pure elastic scattering, *i.e.* the calculation assuming no inelastic scattering and no absorption, the slice transmission function in (1) should be replaced with

$$q_n = \exp(i\sigma U_a \Delta z). \quad (7)$$

Then the calculations based on (5) to (7) will give the pure elastic scattering results of the electron in the crystal. The total scattering intensity calculated with either the total scattering theory or the pure elastic scattering theory will be conserved and equal to each other if no absorption effect is included, so that the calculated absolute reflectances in the two cases can be compared with each other.

It should be pointed out that the spatial variation of U_{ef} in (1) (nonperiodic) does induce an angular

distribution of the inelastic scattering to some extent but does not include any effects of limited coherence range. The action of U_{ef} on the wave may change the average direction of propagation of the electrons, as will be shown in Fig. 2.

3. Computation method

The GaAs (110) surface is assumed to have a perfect structure, so that the atomic arrangement at the surface is the same as that in the bulk. No surface reconstruction or relaxation is considered. The slice thickness is chosen as 2.827 \AA for the [001] azimuth, the electron propagation distance can be calculated by multiplying the slice number by 2.827 \AA . The calculations are performed for 120 kV electrons. A detailed introduction to the computing method is given elsewhere (Wang *et al.*, 1987).

In inelastic RHEED calculations with the multi-slice method (Wang & Lu, 1988), special attention has to be taken to consider the electron feed-in problem on the surface, because the electrons which enter the surface through different surface areas have different mean energy losses when arriving at the exit face of the crystal. This problem can be solved by using the small-beam technique introduced by Wang (1989*b*). A large incident beam is divided into narrow streams, each of which can be considered as a 'monoenergetic' stream with definite energy loss depending on the travelling distance. The total wave function will be the superpositions of all these streams at the definite slice position.

Another problem in RHEED calculation is how far the electron should propagate in order to give the steady-state reflections. According to the calculation results of Wang *et al.* (1989), a mean free travelling distance D can be defined to characterize the path length for interaction of the electrons with the solid, along which most of the electrons travel before being reflected back into the vacuum. This D measures up to 500–700 \AA for GaAs 660 reflections. Therefore, it is necessary to calculate up to the 400th slice in order to get the steady-state propagation. In the following calculations, the incident beam is formed by a window function, the width of which determines the size of the beam. The beam size is chosen large enough, so that no beam cut-off takes place in the considered slice range.

4. Calculation results

Shown in Fig. 1 is a set of calculated RHEED intensities across the 660 specular reflection spot of GaAs (110) for different incident angles. The displayed intensity is normalized with respect to the total intensity of the initial incident beam (I_0), so that the magnitudes of I/I_0 can be compared with each other. The reflection intensities calculated by using the total

scattering theory [(1)] and using the pure elastic scattering theory [(7), without absorption] are represented by the dashed and the solid lines, respectively.

At the exact Bragg-angle incidence, $\theta = 26.5$ mrad for 660 (Fig. 1a), the intensity calculated with the total scattering theory is about 40% stronger than that with the pure elastic scattering theory. When the incident angle is decreased to 24.5 mrad (Fig. 1b), both theories give about the same output except that a slight peak shift (0.8 mrad) is visible.

When the incident angle is changed to 23.5 mrad (Fig. 1c), a large increase of the intensity calculated by using the total scattering theory is seen. This shows that the inelastic scattering can greatly enhance the reflection at some specific angles. It was reported by Wang *et al.* (1989) that the surface potential trapping resonance (elastic) happens only for the 23.5 mrad incident case. This indicates that the incidence at 23.5 mrad corresponds to the strongest resonance excitation of the surface; the inelastic scattering then dominates the resonance process.

With the decrease of the incident angle (Fig. 1d), the reflection intensity calculated using the total scattering theory decreases quite significantly. When the incident angle reaches 21.5 mrad (Fig. 1e), the reflection intensity calculated using the pure elastic scattering theory is much stronger, which is a change in the opposite direction to that for Fig. 1(c). This suggests that the inelastic scattering and the elastic scattering have their strongest resonance states at different

incident angles. Hence the reflected electrons with and without energy losses are not expected to be distributed uniformly in the 660 reflection disk, provided with a convergent beam incidence. This phenomenon has been observed experimentally (see § 6).

The calculated reflectance for the specular reflection spot is plotted in Fig. 2 for different incident angles according to the results in Fig. 1. Several features are shown in Fig. 2. First, the inelastic scattering can quite significantly increase the reflectance of a surface. The maximum observed reflectance is about twice as large as that calculated for pure elastic scattering without absorption (Wang, 1989b). Secondly, a relative shift of the peak positions between the results calculated with the total scattering theory and the pure elastic scattering theory is visible. This shift is a reasonable result of considering the effects of energy loss and the effective potential (Wang, 1989b). It follows from the nonuniform excitation of the elastic and inelastic scattering in the RHEED that the inelastic scattering can change the average direction of propagation of the reflected electrons. The last feature is that about 24% of the incident electrons may be specularly reflected under the surface resonance condition. In off-resonance cases, only about 4–5% of the electrons are specularly reflected. The reflected intensity of the specular 660 spot is expected to increase about six times when set at the resonance condition compared to that set at off resonance. This is shown in the experimental observation in Fig. 4.

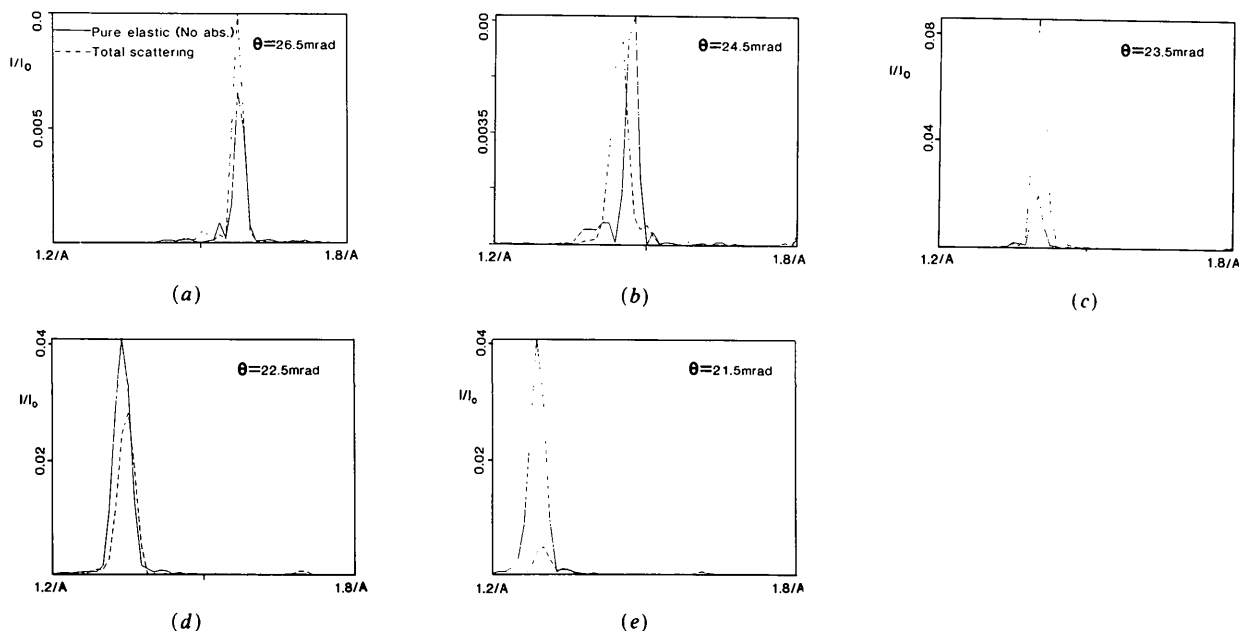


Fig. 1. Calculated RHEED intensities of the GaAs (110) surface across the specular reflection spot for different incident angles. The solid and dashed lines represent the results calculated with the pure elastic scattering theory (without absorption) and the total scattering theory respectively. The displayed intensity I/I_0 has been normalized with respect to the initial incident beam.

The multislice calculation makes it possible to trace the build-up process of the reflection wave. Shown in Fig. 3 is a plot of the calculated intensity ratio of the specular reflection, calculated with the total scattering (I_t) and pure elastic scattering (I_e) theories, *versus* the slice positions. When the electrons propagate for short distances (less than 100 slices), the inelastic scattering effect can be neglected. When the propagation distance is close to the electron inelastic mean free path, ranging from about 700 to 1000 Å, the inelastic scattering becomes significant, resulting in the increase of the ratio I_t/I_e . When the travelling distance becomes larger than the mean travelling distance D (about 500–700 Å) (Wang *et al.*, 1989), along which most of the electrons travel before being reflected back into the vacuum, the ratio I_t/I_e begins to arrive at its steady level.

5. Experimental method

Microdiffraction and scanning reflection electron microscopy (SREM) experiments were performed in a VG HB5 scanning transmission electron microscope (STEM). The vacuum at the specimen stage was about $1.3 \mu\text{Pa}$ or less. The incident beam was 10–15 Å in

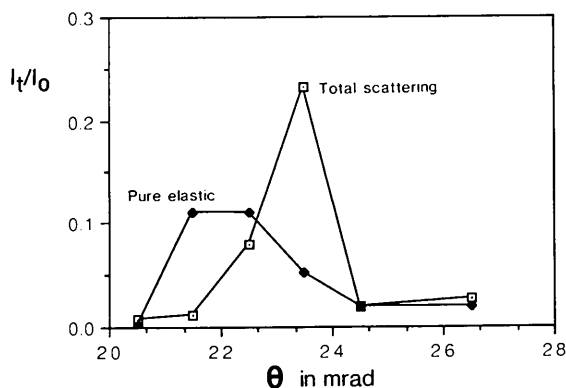


Fig. 2. Calculated rocking curve for the specular reflection spot according to the results in Fig. 1.

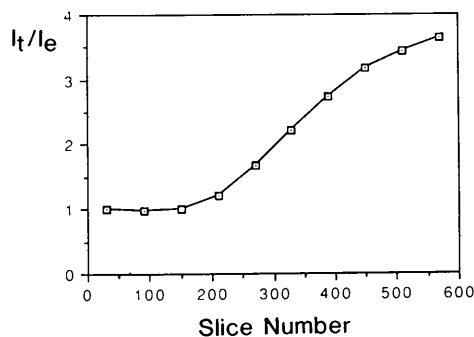


Fig. 3. Intensity ratio of the specular beam, calculated with the total scattering (I_t) and pure elastic scattering (I_e) theories, *versus* the slice position, for incidence $\theta = 23.5$ mrad in Fig. 1(c).

diameter. The REELS spectra were acquired from the reflected spot with a Gatan 607 EELS spectrometer with an energy resolution of about 2.5 eV. The collection angle of the spectrometer was about 2 mrad. The EELS data were recorded with a Kevex data analysis system. The GaAs (110) surface was obtained by cleaving a bulk GaAs crystal in air and was mounted on a double-tilting cartridge. The microscope was operated at 100 kV with beam current density between 10^4 and 10^5 A cm^{-2} .

6. Experimental results

In RHEED geometry, there are two contributors to the plasmon excitation (Wang & Egerton, 1988). One contributor is the excitation of the plasmons while the electrons are approaching and departing from the surface in the vacuum (direct reflection), which is a fixed term for a fixed incident angle and does not depend on the propagation status of the electrons in the surface. Thus, there is always a constant component for plasmon excitation owing to the existence of this term. The other contributor is the excitation of the plasmons while the electrons are resonantly propagating along the surface. The variation of this contribution reflects the resonance propagations of the electrons at the surface.

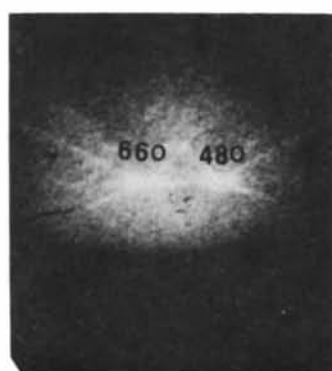
Shown in Fig. 4 is a comparison of the RHEED intensities of the GaAs (110) surface while on (Fig. 4a) and off (Fig. 4b) the resonance. The reflected intensity of the whole pattern is enhanced under the resonance condition. The variation of the intensity in the 660 reflection spot can be measured through the REELS spectrometer. The result shows that the intensity increases about a factor of five to six in Fig. 4(a) compared with that in Fig. 4(b). This is in agreement with the evaluation of Fig. 2.

6.1. REELS observations of electron inelastic scattering and surface resonance

The 660 spot displayed in Fig. 4(a) is not a uniform disk in intensity owing to the convergent incidence of the beam. Shown in Fig. 5(a) is a 660 spot obtained with a smaller objective aperture. Two intensity domains are seen to dominate the 660 disk, separated by about 3–4 mrad and corresponding to the reflection for different incident angles. The inelastic excitation of the surface can be seen through the REELS spectra acquired from the domains *a* and *b*, as shown in Fig. 5(b). The spectra are displayed by normalizing the heights of the zero-loss peak, so that the relative increase of the plasmon-loss part can be considered as the relative increase of the inelastic excitations. In the spectrum acquired from domain *a* (dashed line), the ratio of the total inelastically scattered electrons to the elastically scattered electrons is greater by about 50% compared with that for domain *b* (solid line).

Also, stronger multiple inelastic scattering is visible in the tail part of curve *a*. The results in Fig. 5(b) can be considered as corresponding to the theoretical predictions shown in Figs. 1(c) and (e). Then reflection in domain *a* is mainly dominated by the inelastic resonance scattering; reflection in domain *b* is mainly dominated by the elastic resonance scattering after taking off the contribution from the 'direct' reflection. By elastic resonance we mean that the reflection intensity is enhanced but with less inelastic excitations. By inelastic resonance we mean the strong excitation of the plasmon losses together with the enhancement of the reflection intensity, which is postulated to be due to the propagation of the electrons along the surface, and may be called the 'true' surface resonance.

Whether the domain *a* or *b* is dominated by the elastic or inelastic resonance scattering is critically dependent on the initial incident conditions. If the beam is tilted by about 0.5 mrad away from the orientation of Fig. 5(a) in either direction, then the inelastic excitation behavior in the domains *a* and *b* is switched. Also, in some of the experimental cases,

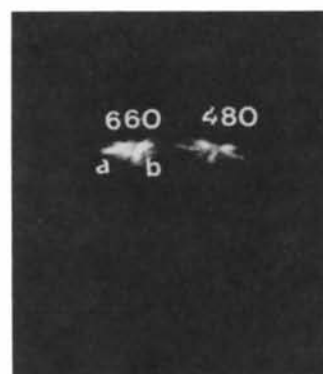


(a)

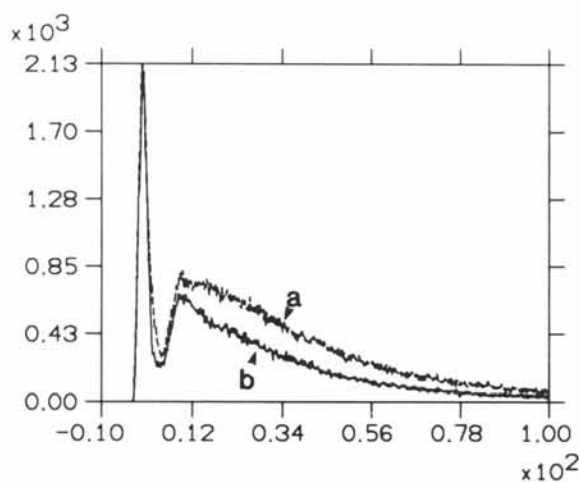


(b)

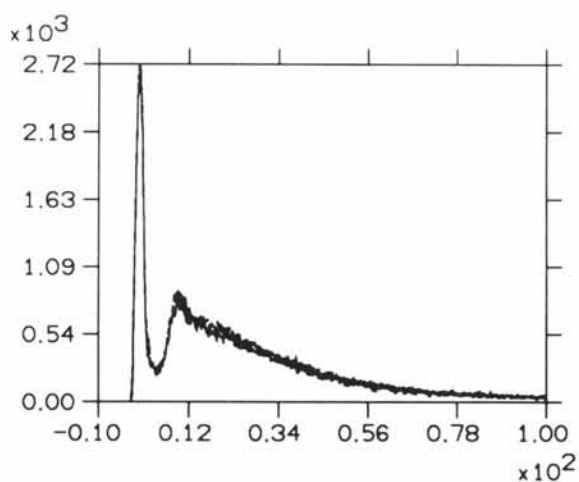
Fig. 4. RHEED patterns from a GaAs (110) surface (a) on the resonance and (b) off the resonance condition.



(a)



(b)



(c)

Fig. 5. (a) RHEED pattern from a GaAs (110) surface. (b) A comparison of the spectra acquired from the domains *a* and *b* in (a). (c) A comparison of the spectra acquired from the domains *a* and *b* but with slightly different resonance conditions.

the diffraction conditions appear to be almost exactly the same as shown in Fig. 5(a), but the inelastic excitation results are totally different from that shown in Fig. 5(b). Fig. 5(c) shows an example of this case. No obvious difference is seen in the spectra acquired from the two domains. These experimental results together with the calculations in § 4 (Fig. 1) indicate that, for small changes of incident angle, the diffraction intensity may not change too much but the excitation processes may be totally different.

To demonstrate the sensitivity of the elastic and inelastic resonances to the diffraction conditions, Fig. 6(c) shows a comparison of the spectra acquired from the 880 spot in Figs. 6(a) and (b). The only difference between Figs. 6(a) and (b) is a slight change of the diffraction conditions, which can scarcely be seen in the diffraction pattern. But the spectra show some significant changes in the plasmon-loss part. This indicates that the resonance propagation of the electrons increases the inelastic excitation, which feeds back and increases the reflectance of a surface according to Fig. 2.

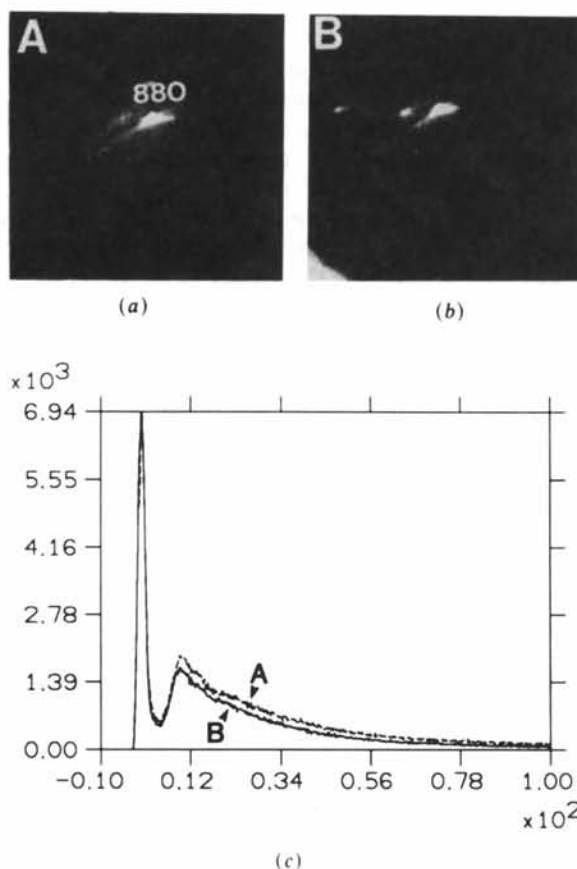


Fig. 6. (a), (b) RHEED patterns from the GaAs (110) surface under slightly different diffraction conditions with the 880 specular reflection. (c) Comparison of the spectra acquired from the 880 spots for A and B. The units of energy loss are eV.

All the above observations are in good agreement with the calculated results in § 3, which, on the other hand, confirms that the theoretical treatment from (1) to (6) (Wang, 1989a) can reasonably characterize the electron inelastic behavior in RHEED.

6.2. An energy-loss peak due to resonance

As shown in Fig. 5(b), the resonance propagation of the electrons at a crystal surface can significantly increase the inelastic excitations of the surface. It is expected that the resonance energy loss of the electrons could be seen in this process. By resonance energy loss we mean that the extra energy loss of the electrons is due to their resonance propagation along the surface. Fig. 7 shows a REELS spectrum acquired from the 660 spot with domain *a* strongly excited [‘true’ resonance condition, see Fig. 5(a)]. Besides the single (11 eV) and the multiple surface plasmon excitations, an extra peak, located at 4.5 ± 0.3 eV, is seen. This peak does not appear in the spectra acquired from either the domain *b* (Fig. 5a) or the 480 reflection spot. When the same experiments were repeated for slightly different diffraction conditions, the peak was observed from the domain *b* but not from the domain *a*. This corresponds to the discussion in the last section about the critical dependence of the surface resonance on the diffraction conditions. Hence, this indicates that the observed peak must be related to the inelastic resonance propagations of the electrons along the surface, which disappear if the ‘true’ resonance conditions are not met.

For the GaAs (110) surface, an extra peak, located at 6.3 eV, has been observed by Peng & Cowley (1988), but the peak intensity appears about ten times stronger than the elastic zero-loss peak, which seems

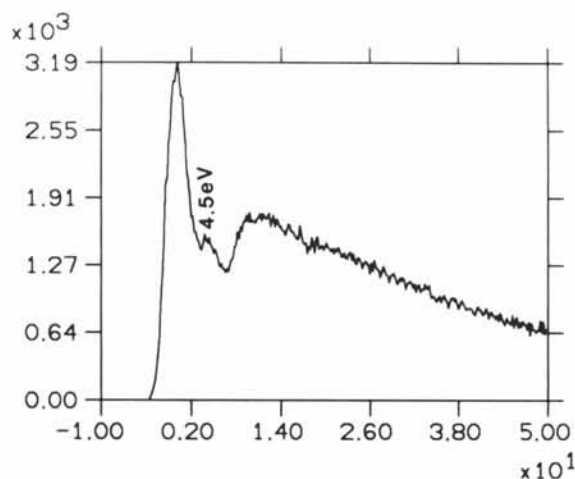


Fig. 7. REELS observation of the resonance energy-loss peak at the GaAs (110) surface. The spectrum was obtained from domain *a* in Fig. 5(a) for the 660 specular reflection. The units of energy loss are eV.

quite abnormal. Also, they have shown that the peak position shifts to about 8.9 eV after the surface is contaminated. However, our observation shown in Fig. 7 indicates that the peak intensity is about 1/15 of the zero-loss peak or about 0.5–1% of the total spectrum; the peak shifts to about 4 eV after the surface is contaminated, which is in the opposite direction to that reported by Peng & Cowley (1988). In their case the incident beam was tilted about 15 mrad away from the principal azimuth in the direction parallel to the surface. Therefore, the peak shown in Fig. 7 might not correspond to the same type of excitation as for their case, which was interpreted as due to channelling radiation from transitions between the intrinsic bound states.

In our observations, one cannot obtain the 'extra' peak if the incident beam is tilted off the 'true' resonance by 1 mrad or even less. This indicates that the peak we observed in Fig. 7 must be related to the surface resonance and is a characteristic of the surface resonance states. This shows that the 'true' surface resonance happens in a very narrow angular range, as predicted theoretically (Wang *et al.*, 1989). The enhancement of the reflection intensity may not be the proper criterion for the occurrence of the 'true' surface resonance.

One of the possible interpretations for this peak is the production of resonance radiation. It has been shown theoretically and experimentally that the surface resonance wave is an oscillating wave while propagating along the surface (Wang *et al.*, 1987; Wang *et al.*, 1989). It is equivalent to an 'oscillator' in space. The acceleration of the electrons in this 'oscillator' can radiate energy. It can be estimated that the radiation probability per cycle of oscillation is about 0.5% (Jackson, 1976). This value is close to the ratio between the extra peak and the whole spectrum in Fig. 7. Also the oscillating energy is of the right order if the oscillating periodicity is a few hundred ångströms.

7. Concluding remarks

The inelastic plasmon diffuse scattering can greatly enhance the reflectance of a crystal surface, and may have a dominant effect in the surface resonance excitation. The inelastic scattering can change the average direction of propagation of the reflected electrons. Within the 660 disk, the inelastic reflections are dominant for some of the angular range, but the elastic reflection takes the dominant role for the reflection in some other angular range. This indicates that the domains which have the strongest inelastic reflection must be the 'true' surface resonance reflections, because the inelastic excitation should be strongly excited while the electrons are propagating along the surface. There is an evanescent wave propagating along the surface under some particular conditions,

which produces the 'true' resonance excitation of the surface. The strong enhancement of the reflection intensity is due to the resonance propagations of the electrons in the intrinsic bound states of the surface (Marten & Meyer-Ehmsen, 1985). The electrons jump out of the resonance probably due to inelastic scattering.

The intensities of the other reflections which are not due to the 'true' resonance reflection are compatible with that of the 'true' resonance reflection but with much less inelastic scattering. This could possibly be interpreted based on the calculations of Bleloch *et al.* (1989). In some particular incident conditions, owing to the double Bragg reflections, most of the reflection intensities accumulate on the specular beam, resulting in the increase of the reflection intensity but less inelastic excitation. This means that the strong enhancement of the reflection intensity due to this process cannot be considered as the resonance reflection. Therefore, the enhancement of the reflection intensity in RHEED may not be the proper indication of the occurrence of the 'true' surface resonance. Also, the 'true' resonance happens at some very particular angles with the angular range less than 1 mrad. Generally, it is not so easy to get the exact 'true' resonance. This is in agreement with the theoretical predicted resonance of the surface potential trapping reported by Wang *et al.* (1989).

An 'extra' peak, located at 4.5 eV, is observed in the REELS study of the 'true' resonance reflection, but not in the studies of the other reflections. This peak is considered as one indication of the 'true' surface resonance. This peak might be related to the resonance radiation of the electrons while propagating along the surface in an oscillating way. The probability of exciting this peak is about 1%.

The good agreement between the theoretical calculations and the experimental observations proves that the theory (Wang, 1989a; Wang & Lu, 1988) of including the inelastic scattering in RHEED calculations can reasonably characterize the total scattering behavior of the electrons at surfaces.

This work was supported by the Office of Naval Research under grant N00014-86-K-0319 (MAPS program) (ZLW) and NSF grant DMR 8510059 (JL), and made use of the resources of the ASU Facility for High Resolution Electron Microscopy, supported by NSF grant DMR 86-11609.

References

- BLELOCH, A. L., HOWIE, A., MILNE, R. H. & WALLS, M. G. (1989). *Ultramicroscopy*. In the press.
- COLELLA, R. (1972). *Acta Cryst.* **A28**, 11–15.
- COWLEY, J. M. (1988). *Acta Cryst.* **A44**, 847–853.
- COWLEY, J. M. & MOODIE, A. F. (1957). *Acta Cryst.* **10**, 609–619.
- GARCIA-MOLINA, R., GRAS-MARTI, A., HOWIE, A. & RITCHIE, R. H. (1985). *J. Phys. C*, **18**, 5335–5348.

- JACKSON, J. D. (1976). *Classical Electrodynamics*, 2nd ed., § 14.2. New York: John Wiley.
- KAMBE, K. (1988). *Ultramicroscopy*, **25**, 259–263.
- KIKUCHI, S. & NAKAGAWA, S. (1933). *Sci. Pap. Inst. Phys. Chem. Res. (Jpn)*, **21**, 256.
- MAKSYM, P. A. & BEEBY, J. L. (1981). *Surf. Sci.* **10**, 423–438.
- MAKSYM, P. A. & BEEBY, J. L. (1982). *Appl. Surf. Sci.* **11/12**, 663.
- MARTEN, H. & MEYER-EHMSEN, G. (1985). *Surf. Sci.* **151**, 570–584.
- PENG, L. M. & COWLEY, J. M. (1986). *Acta Cryst.* **A42**, 545–552.
- PENG, L. M. & COWLEY, J. M. (1988). *Surf. Sci.* **204**, 555–567.
- WANG, Z. L. (1989a). *Acta Cryst.* **A45**, 193–199.
- WANG, Z. L. (1989b). *Surf. Sci.* In the press.
- WANG, Z. L. (1989c). *Surf. Sci.* In the press.
- WANG, Z. L. & EGERTON, R. F. (1988). *Surf. Sci.* **205**, 25–37.
- WANG, Z. L., LIU, J., LU, P. & COWLEY, J. M. (1989). *Ultramicroscopy*. In the press.
- WANG, Z. L. & LU, P. (1988). *Ultramicroscopy*, **26**, 217–226.
- WANG, Z. L., LU, P. & COWLEY, J. M. (1987). *Ultramicroscopy*, **23**, 205–222.

Acta Cryst. (1989). **A45**, 333–337

Concerning Order Parameters in the Statistical Dynamical Theory of Diffraction

BY PIERRE J. BECKER* AND MOSTAFA AL HADDAD†

Laboratoire de Cristallographie, CNRS, and Université J. Fourier, 166X, 38042 Grenoble CEDEX, France

(Received 28 November 1988; accepted 16 December 1988)

Abstract

The development of the statistical dynamical theory of diffraction by real crystals involves two order parameters: a long-range and a short-range one. These parameters play a fundamental role in practical applications of the theory to real diffraction data. A reasonable probabilistic model is proposed to describe the phase correlation at two given scattering positions. This model allows for a tractable solution of the propagation equations for the beams.

Introduction

The propagation of X-rays or neutrons in real crystals can be described by Takagi's equations (Takagi, 1962, 1969; Kato, 1973). For a Bragg reflection associated with the reciprocal-lattice vector \mathbf{h} , let D_0 and D_h be the amplitudes of the waves propagating in the incident direction (with coordinate s_0) and the diffracted direction (with coordinate s_h) respectively. Takagi's equations are

$$\begin{aligned} \partial D_0 / \partial s_0 &= i\chi_{\bar{h}}\varphi D_h, \\ \partial D_h / \partial s_h &= i\chi_h\varphi^* D_0. \end{aligned} \quad (1)$$

In (1) χ_h is given by

$$\chi_h = (\lambda a C / V) F_h \quad (2)$$

where λ is the wavelength, V is the volume of the unit cell, $a = 10^{-12}$ cm for neutrons and 0.28×10^{-12} cm for X-rays, and C is the polarization factor for X-rays. F_h is the structure factor

$$|\chi_h| = 1/\Lambda$$

where Λ is the extinction distance.

The imperfect nature of the crystal occurs through the phase factor φ ,

$$\varphi = \exp [2\pi i \mathbf{h} \cdot \mathbf{u}(\mathbf{r})] \quad (3)$$

where $\mathbf{u}(\mathbf{r})$ is the local displacement from the perfect position \mathbf{r} .

Without a precise knowledge of the distortion field $[\mathbf{u}(\mathbf{r})]$, (1) can only be solved by introducing a statistical hypothesis concerning the distribution of \mathbf{u} within the crystal. Kato (1980) proposed a statistical theory for describing the propagation of the beams in real crystals: this theory covers the whole range between perfect crystals (dynamical theory) and ideally imperfect crystals (kinematical theory). The beams, which are coherent for a perfect crystal, become partially incoherent, owing to phase couplings of the type $\varphi(\mathbf{r})\varphi^*(\mathbf{r}')$ which occur in the expression for the intensities. The statistical properties of the phase factor $\varphi(\mathbf{r})$ are thus essential for developing the theory.

Kato's theory has been modified by the present authors (Al Haddad & Becker, 1988) and then generalized (Becker & Al Haddad, 1989a, b). The purpose of the present paper is to discuss the statistical properties of $\varphi(\mathbf{r})$ and its spatial correlations, since this leads to the fundamental parameters appearing in the integrated reflectivity or in the extinction factor.

* Present address: Laboratoire de Minéralogie et Cristallographie, Université Pierre et Marie Curie, Tour 16, 4 place Jussieu, 75252 Paris CEDEX 05, France.

† Permanent address: Atomic Energy Commission, PO Box 6091, Damascus, Syria.